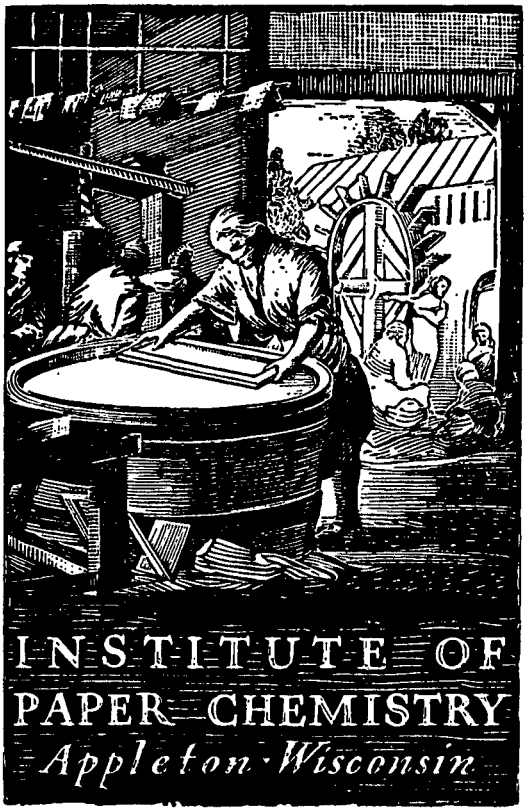

REFINING BY ABRASIVE WEAR OF PULP FIBERS IN SHEAR FLOW

Project 3384

Report Four
A Progress Report
to
MEMBERS OF THE INSTITUTE OF PAPER CHEMISTRY

August 26, 1983

THE INSTITUTE OF PAPER CHEMISTRY

Appleton, Wisconsin

REFINING BY ABRASIVE WEAR OF PULP FIBERS IN SHEAR FLOW

Project 3384

Report Four

A Progress Report

to

MEMBERS OF THE INSTITUTE OF PAPER CHEMISTRY

August 26, 1983

TABLE OF CONTENTS

THE INSTITUTE OF PAPER CHEMISTRY

Appleton, Wisconsin

REFINING BY ABRASIVE WEAR OF PULP FIBERS IN SHEAR FLOW

SUMMARY

When a pulp suspension is sheared between parallel disks, three flow regimes are possible. Which one is realized depends on the shear rate, consistency, and the surface microstructure of the disks. Abrasive wear of pulp fibers has been studied in two of the three regimes. When the flow regime is characterized by the rolling of flocs (regime I), the experiments show that abrasive wear is negligible. However, abrasive wear is important when the suspension is mobilized (regime III) and fiber-surface interactions are frequent. The key parameters in this regime are the shear rate, the scale of the surface roughness of the disks, and to a lesser extent, consistency. In particular, we have found that the number-average fiber length is reduced linearly with the maximum average shear rate.

The transition between rolling flocs and mobilized flocs is a flow regime characterized by an admixture of rolling flocs, immobilized flocs, and mobilized flocs. Although abrasive wear of pulp fibers in this regime was not studied, the amount of wear is expected to be less than that in regime III because of the lack of dispersion and mobility of the flocs.

The application and significance of the foregoing results in papermaking operations are inextricably linked to the rate of abrasive wear. Our experiments show that abrasive wear can be substantial even after 2 minutes, given certain flow conditions. For example, when pulp was sheared for 2 minutes with 120 grit and a maximum average shear rate of 2000 sec^{-1}, the number-average fiber length was reduced by 40% and the z-average fiber length by about 20%. The photomicrographs of the abraded pulp showed substantial evidence of external fibrillation (reduced

freeness). Also, it is reasonable to expect that these results will be magnified at high shear rates. Thus, papermaking operations that require pulp to be recirculated or transported in corroded pipe lines over long distances at average shear rates in excess of 2000 sec^{-1} are candidates for abrasive wear.

Abrasive wear, as we have shown, can have a beneficial effect on pulp strength properties. If abrasive wear is promoted, it is possible to refine pulp at shear rates much lower than previously reported. Significant refining action was achieved at shear rates of about 2000 sec^{-1} (Table II), whereas previous experiments by Waterhouse (1) and by Westman (2) were at shear rates about two orders of magnitude greater. Further, the plate clearance in our work was never less than 1.9 mm, whereas in their experiments the clearance was of the order of 0.2 mm or less.

The foregoing results make apparent the importance of surface microstructure in shear refining. Although it is well known that the material used in the manufacture of refining plates influences the performance of refiners, a fundamental explanation for the observed differences in performances has not been given [Bridge and Hamer (3)]. The abrasive wear experiments described in this work provide a convenient method for investigating the effect of surface microstructure on external fibrillation under controlled conditions and in the absence of fiber cutting due to bar crossings.

INTRODUCTION

When surfaces are pressed together by a normal force, surface interaction phenomena such as friction, lubrication (boundary and hydrodynamic), and adhesion become important and often must be accounted for in order to fully appreciate and understand the dynamics and kinematics of the contact process [Bowden and Tabor (4)]. In papermaking this is all too true. It is known, though perhaps not widely appreciated, that surface interaction phenomena play a crucial role in unit operations such as drying, creping, wet pressing, and refining [Casey (5)]. Some of the unique properties of pulp suspensions are also a result of interfacial contact brought about by fiber-fiber and fiber-wall interactions. Network strength is one property in particular [Wahren (6)].

A natural consequence of interfacial contact is wear. It is generally accepted that there are four forms of wear when surfaces come into contact [Rabinowicz (7)]: adhesive, abrasive, corrosive, and surface fatigue. Adhesive wear occurs when a smooth surface slides against another smooth surface and fragments are pulled off one surface to adhere to another. Abrasive wear occurs when a rough, hard surface slides against a softer surface and plows out fragments from it. Factors that contribute to abrasive wear rate are abrasive particle size, abrasive hardness, the sliding velocity, and the presence of a lubricant [Rabinowicz (7)]. Abrasive wear can also occur as an indirect consequence of corrosive wear. This occurs when corrosion products in the form of particles are trapped between two surfaces in relative motion. Surface fatigue is similar in many respects to the phenomenon called fatigue failure which occurs when materials are subjected to the cumulative action of stress cycles. Indeed, the principle of fatigue failure is used to good advantage in the manufacture of mechanical pulp where wood chips and fibers are subjected to reverse shear and compression cycles [Atack (8)].

Pulp suspensions when sheared can show signs of wear. The change in freeness that occurs when a pulp is subjected to excessive pumping is a familiar sign to many mill operators. However, as far as we know, there is no quantitative study in the literature of wear in pulp suspension flows and the factors that influence it. Because adhesive wear is reduced considerably in the presence of a lubricant, it is unlikely that adhesive wear is of importance in pulp suspensions, especially at consistencies less than 10%. (A possible exception is when the suspension is subjected to excessive normal forces.) On the other hand, it is not too difficult to imagine conditions favorable for abrasive wear.

In this paper we report on an experimental study of abrasive wear in pulp suspension flows at consistencies less than 5 percent. Specifically, we report the change in the fiber length distribution of the pulp as a function of consistency, floc mobility, rate of shear, and surface roughness. Microscopy is used to obtain a qualitative measure of the types of changes that occur in the fiber as a result of abrasive wear. Much of the motivation for this work stems from our ongoing research in the refining of chemical pulp. Indeed, the results from this research show that there are flow conditions that accentuate abrasive wear of pulp fibers, and the resulting changes in fiber morphology have a beneficial effect on pulp properties, i.e., strength properties of the pulp are enhanced. Furthermore, these refining effects are achieved at shear rates about two orders of magnitude lower than those previously reported for refining.

EXPERIMENTAL PROCEDURE

For abrasive wear to occur in pulp suspension flows, the fibers must make contact with the abrading surface and move relative to it when contact is made. Thus, central to the understanding of abrasive wear is knowledge of the flow characteristics of the suspension when sheared.

To date most of our understanding of pulp suspensions flows is derived from pressure drop measurements in pipe flow coupled with flow visualization [Norman et al. (9)]. Unfortunately, the constitutive law that relates bulk stress of a suspension to flow kinematics and fiber dispersion is not well understood. This means that pipe flow data are often of little help in predicting suspension flow characteristics in other flow geometries. Abrasive wear experiments in pipe flow have the disadvantage that the residence time distribution of the fibers is a function of flow conditions, which makes interpretation of the results difficult. Therefore, in this study a batch flow system was chosen in which the flow characteristics could easily be determined. A schematic of the experimental apparatus is shown in Fig. 1.

The rotor was made from stainless steel and was driven by a 1/2 hp variable speed motor. Rotor speeds of up to 1100 rpm were possible. The stator, made from Plexiglas to aid flow visualization, was threaded into a steel housing which was loaded against the rotor through a Teflon seal. The internal diameter of the chamber so formed was 102 mm. The threads in the housing allowed the clearance between the rotor and stator to be adjusted at will. Typically, the plate clearance was varied between 1.9 and 9.5 mm.

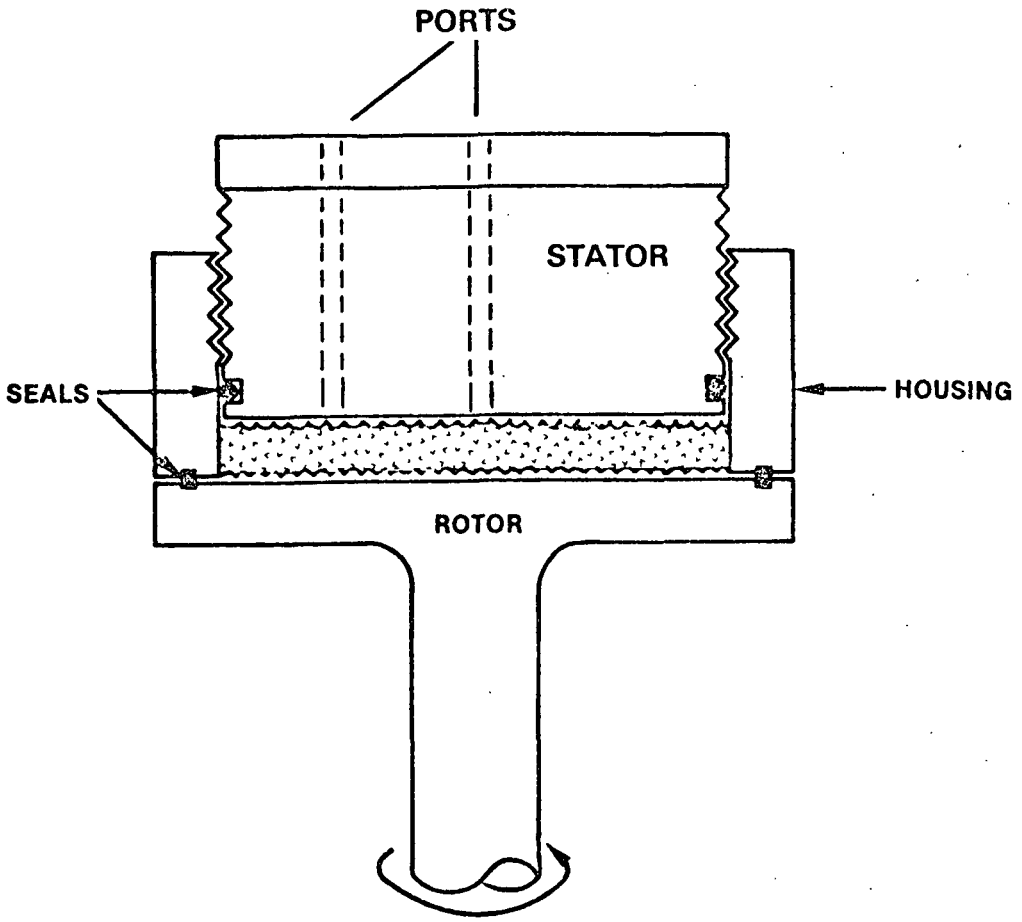

Figure 1. Schematic of the apparatus; stator diameter = 102 mm.

To aid the removal of any air bubbles that were trapped in the chamber after the addition of pulp, two ports were located in the stator, one of which was at the center. When the suspension was sheared, the trapped air bubbles migrated toward the chamber center, where they were removed through the center port by displacement with water introduced at the outer port.

To promote abrasive wear the roughness of the rotor/stator surfaces was altered by attaching silicon carbide sandpaper with various grit sizes. The sandpaper used ranged from a 400 grit, which had a grit size of approximately 38 μm or less, to 60 grit, which had a grit size of 240 μm or less.

The flow characteristics of a softwood pulp suspension when sheared in the apparatus were determined by flow visualization. The various flow regimes were mapped out as a function of the system parameters. The parameters varied were rotor speed, plate clearance, consistency, and surface roughness.

Two softwood pulps were used in the experiments. In the abrasion experiments an unbleached sulfite pulp was used and prepared as follows: Lap pulp was soaked for 48 hours and thereafter dispersed for 2 1/2 minutes in a British disintegrator. Following this the pulp was screened in a Bauer-McNett classifier. The fraction retained by the #14 mesh screen was oven dried, and then required amounts were accurately weighed out and redispersed in known amounts of water. Classifying the pulp ensured that the fiber length distribution of the unsheared pulp was sufficiently narrow so that small changes in fiber length due to abrasive wear could easily be detected. In the refining experiments a bleached kraft pulp was used. Its preparation was the same as for the sulfite pulp except it was not classified.

FIBER LENGTH ANALYSIS

The fiber length distributions were measured with The Institute of Paper Chemistry semiautomatic length recorder. The recorder divides the measured fibers into length groups (0.2 mm intervals), and automatically gives the number of fibers in each group, as well as the total number of measured fibers. About 600 fibers were measured for each fiber length analysis.

In the analysis of the data it is convenient to represent the fiber length distribution in terms of moments of the distribution. Specifically we define number-, weight-, and z-average lengths by

$$\overline{L}_n = \sum F_i \overline{L}_i / \sum F_i$$

$$\overline{L}_w = \sum F_i \overline{L}_i^2 / \sum F_i \overline{L}_i$$

$$\overline{L}_z = \sum F_i \overline{L}_i^3 / \sum F_i \overline{L}_i^2$$

Here F_i is the class frequency (%) and $\overline{L}_i$ the class average fiber length. The index i is summed from 1 to m, where m is the number of length classes. It follows from the definitions of $\overline{L}_w$ and $\overline{L}_n$ that $\overline{L}_w \geq \overline{L}_n$. The equality of $\overline{L}_w$ and $\overline{L}_n$ corresponds to a sample of uniform length. Thus the ratio $\overline{L}_w/\overline{L}_n$ is a measure of the width of the distribution or polydispersity in fiber length. The fiber averages defined above are analogous to the average molecular weights defined by the polymer chemist.

Since the number-average fiber length is very sensitive to changes in the number of small fibers present, it is a convenient index for monitoring changes in fiber length distribution due to abrasive wear. Indeed, its sensitivity to the number of small fibers present is the reason why it is not used for correlating sheet properties [Clark (10)].

FLOW VISUALIZATION

When a pulp suspension is sheared between parallel disks, we are able to discern three floc structures with distinct mobilities. They are rolling flocs, immobilized flocs, and mobilized flocs. In this work immobilized flocs are defined as those flocs that adhere indefinitely to either the rotor or stator. In contrast, mobilized flocs are those that undergo continuous slip-stick motion, i.e., they do not adhere preferentially to either the rotor or stator. Based on these observations it is convenient to define three flow regimes that account for all possible floc structures. When the flow consists of rolling flocs only, it is termed regime I; when it consists of mobilized flocs only, it is termed regime III; and when it consists of an admixture of rolling, immobilized, and mobilized flocs, it is termed regime II. Floc size distribution in the three regimes is determined by the rate of shear (or more precisely the power dissipation per unit mass of dry fibers), the microstructure of the plate surfaces, and the consistency. Note, our classification of the flow regimes resembles that given by Robertson and Mason (11) and others for pipe flow, as it undoubtedly must.

REGIME I

At a given plate clearance and at low rotor speeds there is a critical consistency at which immobilized flocs form. When the consistency is less than the critical value, rolling occurs soon after the rotor is set in motion. Initially an assortment of cylindrical rolls of different lengths are formed. The rolls tend to align along rays emanating from the rotor center. Each roll rotates about its major axis and about the rotor axis; the angular velocity of the roll about the rotor axis is apparently a function of its length and density.

After rolling commences the rolls do not keep their relative positions. The longer and denser rolls tend to overtake their less dense and shorter companions. When rolls collide, one of two possibilities can occur: they can combine to form a longer and denser roll, or they can deform and slide over each other. The latter possibility tends to occur when one of the colliding rolls is much denser than its collision partner.

At constant rotor speed it is possible after a short period of time (1-5 minutes) to end up with one large dense roll, the aftermath of many collisions. Although at this point the roll is still cylindrical in cross section, it is generally tapered along its length, with its wide end nearest the chamber wall. When the orientation, size, and symmetry of the roll remains constant with time, it is termed an equilibrium roll, an example of which is shown in Fig. 2.

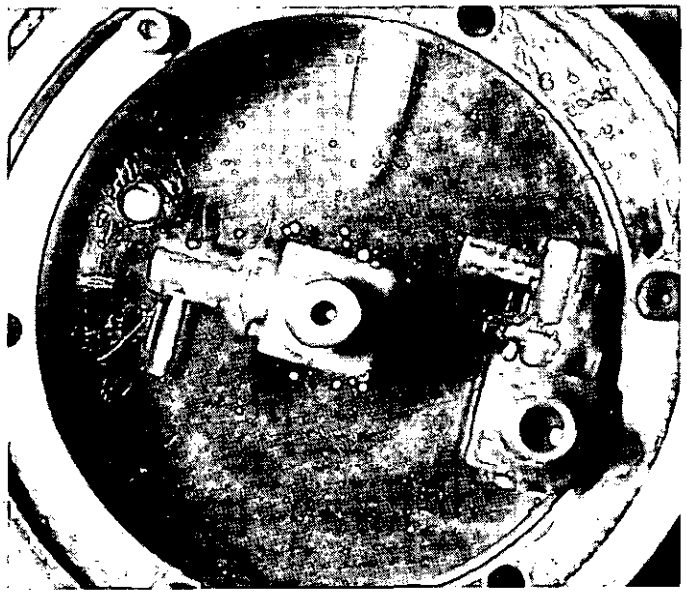

Figure 2. An equilibrium roll formed at a rotor speed of 67 rpm, a plate clearance of 8.9 mm, and a consistency of 0.05%.

Careful observation of the liquid surrounding the equilibrium roll reveals the presence of loose fibers, but the concentration of these fibers seems too low to allow the formation of an additional roll or a roll that has the necesary network strength to coexist with the equilibrium roll. Generally speaking, at fixed plate clearance the density of an equilibrium roll increases with consistency until a consistency is reached beyond which it is impossible to form a single equilibrium roll. Then, instead, multiple equilibrium rolls are formed.

When multiple equilibrium rolls are present, increasing the consistency leads to an arbitrary partition of the available new fiber among the various rolls. In such instances no general trends can be stated about the density of a particular roll as the consistency is increased up to the critical value. However, once the critical value is exceeded, immobilized flocs are formed and rolling is impeded.

REGIME III

Mobilized flocs result from the disruption of either equilibrium rolls or immobilized flocs when the rotor speed or power dissipation is increased. The first sign of disruption of an equilibrium roll is the loss of fibers at its wide end, i.e., near the side wall. This generally results in a loss of axial symmetry of the roll, which gives rise to new elongated shapes. Final disruption is characterized by the complete breakdown of the roll.

In the case of multiple equilibrium rolls, the disruption process is more complicated. Once a roll starts to disrupt its angular speed about the rotor center changes, and collisions with other rolls are possible. This leads to the formation of flocs which become immobilized on the rotor or stator surface. The immobilized flocs can be dislodged from the plate surfaces, i.e., mobilized, by a further

increase in speed. The speed at which there are no longer any immobilized flocs or rolls present in the chamber defines the onset of flow regime III.

In Fig. 3 we show the flow regimes possible for various combinations of rotor speed and consistency when the plate clearance is 6.35 mm and with silicon carbide sandpaper (240 grit) attached to both the rotor and stator. To observe the flow regimes ten equally spaced segments were cut out of the sandpaper disks. The dashed line separating regime I and II gives approximately the variation of the critical consistency with rotor speed at fixed plate clearance. The effect of surface roughness on the flow regimes is predictable insofar as surface roughness promotes rolling and floc mobilization. For example, if the sandpaper on the stator is removed regime II in Fig. 3 is increased at the expense of regimes I and III. This is illustrated in Fig. 4 which shows the flow regimes possible when the stator surface is smooth and the rotor speed is 100 rpm. (Compare flow regime boundaries in Fig. 3 and 4 at the same rotor speed and plate clearance.) The solid curve separating regime I and II defines the critical consistency but this time as a function of plate clearance at fixed rotor speed. It is noteworthy that the critical consistency decreases with plate clearance, and when the plate clearance is less than the average fiber length, i.e., < 3 mm, the consistency range for rolling to occur is diminished appreciably.

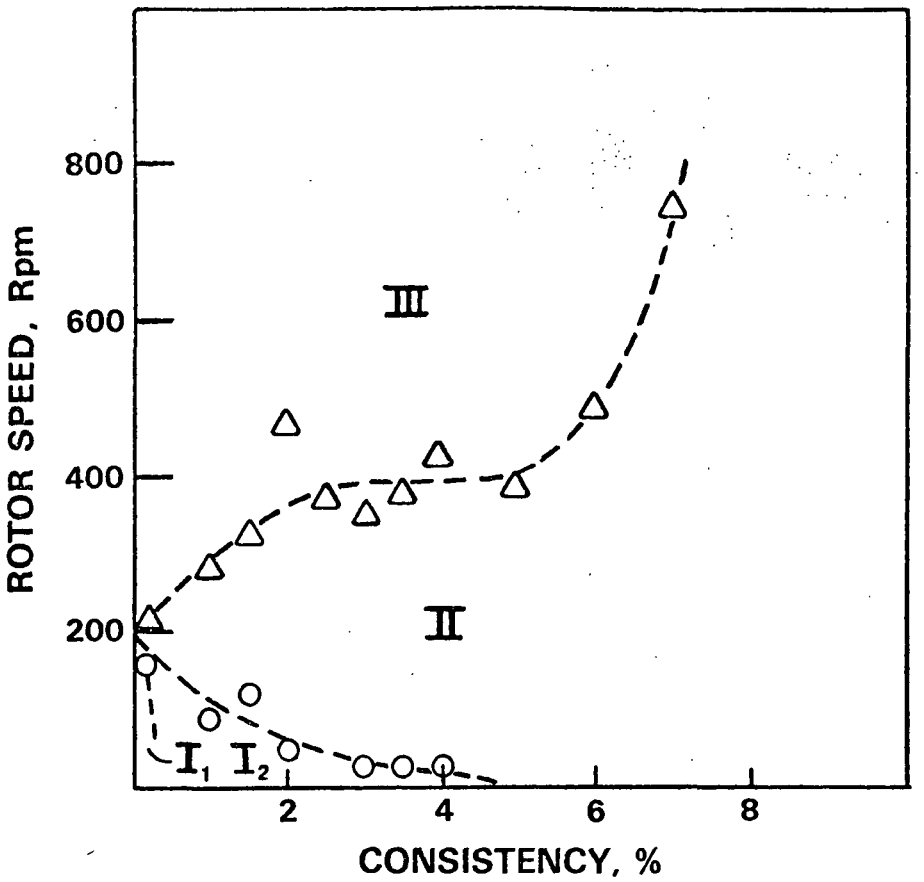

Figure 3. The flow regimes at fixed plate clearance (6.35 mm); single rolls (I_1); multiple rolls (I_2); admixture of rolls, mobilized flocs, and immobilized flocs (II); mobilized flocs (III).

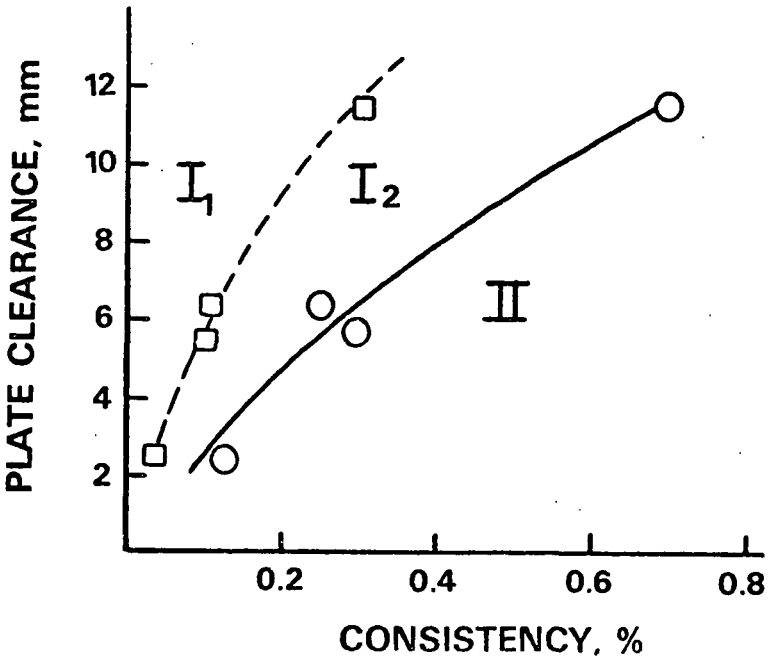

Figure 4. The flow regimes at fixed rotor speed (100 rpm); single rolls (I_1); multiple rolls (I_2); admixture of rolls, mobilized, flocs and immobilized flocs (II).

ABRASIVE WEAR IN REGIME I

When an equilibrium roll is formed in regime I, there is little evidence of fibers aligned and twisted along the major axis of the roll. This suggests that the roll is not subjected to a twisting moment about its ends and that it simply rotates abouts its major axis as if it were a solid body. (Twisted fibers aligned along the roll axis become evident when the plate clearance is less than the average fiber length, a situation not considered here.) Since the tangential velocity at the rotor surface increases radially outwards, solid body rotation is achieved only if (i) the roll makes contact with both the rotor and stator surfaces at the same radial position or (ii) the roll makes contact at more than one radial position but the frictional force at the rotor surface varies with radial position, i.e., the roll slips at the rotor surface. Recall slip is crucial if abrasive wear is to occur during rolling [Bowden and Tabor (4)].

The kinematics of a fiber roll can be best appreciated by analyzing a cross section of a roll at some radial position r_D from the rotor center, as shown in Fig. 5. If V_A is the tangential speed of the center of mass of the roll cross section at r_D, and $\underset{\sim}{R}_D$ is the position vector denoting the point of contact at the rotor surface, then it follows from standard kinematic arguments [Symon (12)] that

$$\frac{d\underset{\sim}{R}_D}{dt} = V_A\underset{\sim}{i} + (\underset{\sim}{\omega} \times \underset{\sim}{r}) \qquad (1)$$

where $\underset{\sim}{\omega}$ is the angular velocity of the fiber roll abouts its major axis. If there is no slip at position r_D, it is readily shown that (1) reduces to the familiar result for normal rolling [May et al. (13)]:

$$V_D = 2\ V_A = r\omega\ 2\ r\omega_D \qquad (2)$$

where V_D is the tangential speed of the rotor surface at the point of contact. This relation can be expressed in terms of the angular velocity of the rotor, ω_D, and the angular velocity of the fiber roll about the rotor center, ω_A:

$$\frac{\omega_A}{\omega_D} = 0.5 \tag{3}$$

Note the point of contact does not appear explicitly in either (2) or (3); to determine it requires knowing the angular velocity of the roll abouts its major axis. If a is the radius of the roll, it follows from (2) and (3) that the point of contact is given by $r_D = a\,\omega_A\,\omega$.

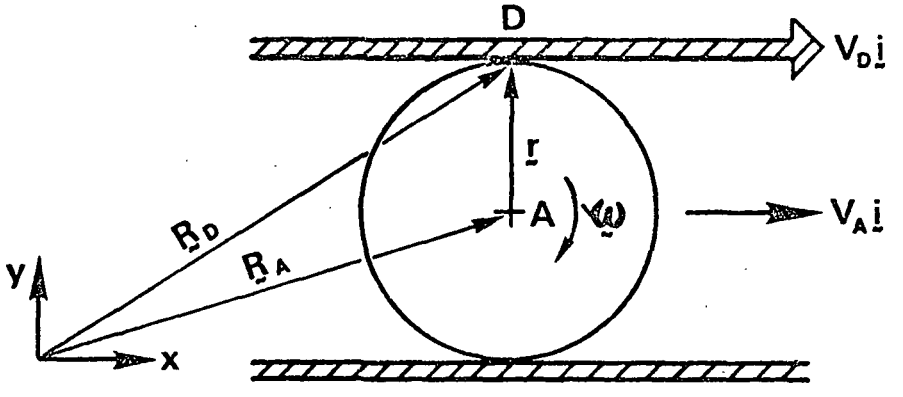

Figure 5. Cross section of fiber roll at radial position r_D.

When slip takes place at the point of contact, Eq. (3) is no longer valid. Possible factors that can contribute to slip are hysteresis losses due to elastic deformation of fibers in the roll [Bowden and Tabor (4), May et al. (13)] and the presence of a lubricating liquid film between the roll and the rotor surface.

To test whether normal rolling occurs in regime I, a series of experiments was carried out with bleached softwood kraft pulp. The angular velocity of the roll about the rotor axis, ω_A, was measured as a function of the rotor speed, ω_D, for different plate clearances and consistencies. Measurements were taken only after the roll had achieved an equilibrium configuration, as described in the Flow Visualization Section. To promote rolling, sandpaper (240 grit) was affixed to the rotor surface.

Typical results are shown in Fig. 6. The plate clearances and consistencies chosen for the experiments were representative of regime I (see Fig. 4). When the plate clearance is of the order of the average fiber length, i.e., 3.81 mm, the measured value of ω_A/ω_D is 0.5 to within one percent. This is the value predicted for normal rolling. When the plate clearance is increased to 6.35 mm ω_A/ω_D is slightly less than 0.5 and remains approximately constant over a wide range of rotor speeds. The latter result suggests that there is a small amount of slip at the point of contact or elsewhere at the rotor surface. It was not possible to determine the cause of slip from the experiments.

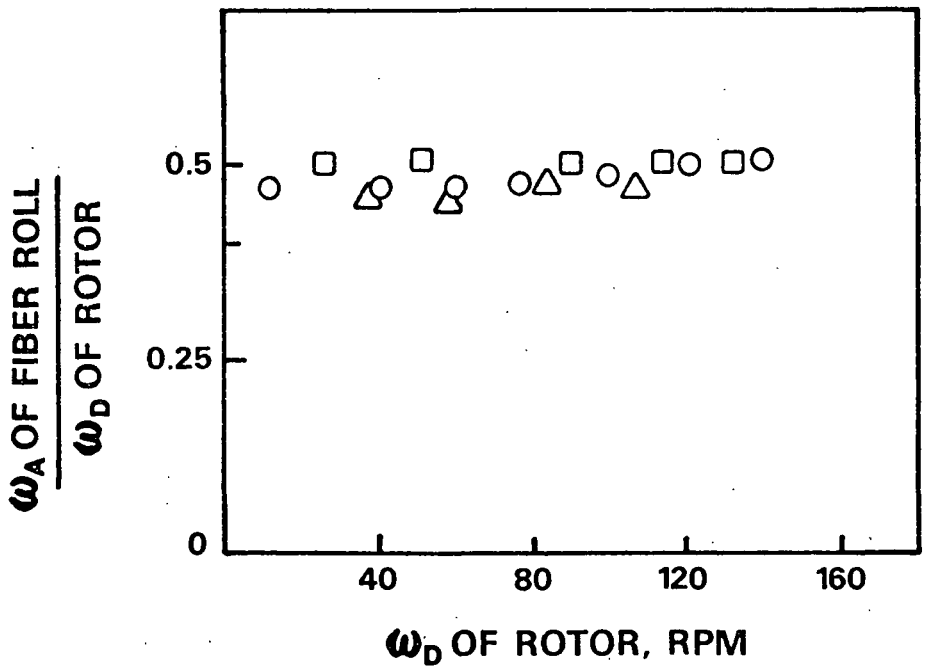

Figure 6. Angular velocity of fiber roll about rotor center (ω_A) as function of rotor speed (ω_D); □ plate clearance = 3.81 mm, consistency = 0.05%;) plate clearance = 6.35 mm, consistency = 0.05%; Δ plate clearance = 6.35 mm, consistency = 0.10%.

To determine whether fibers experienced any abrasive wear from rolling, SEM photomicrographs were made of pulp specimens taken from a fiber roll after 7 minutes of rolling. The roll was formed at 70 rpm at a consistency of 0.05% and a plate clearance of 6.35 mm with silicon carbide sandpaper (240 grit) attached to the rotor. The measured value of ω_A/ω_D was 0.48. Displayed in Fig. 7 are representative SEM photomicrographs of pulp specimens (i) after and (ii) before rolling. The photomicrograph taken after rolling shows some evidence of abrasive wear as external fibrillation, but the amount is small. There was also no measurable change in the fiber length distribution. Fibers subjected to rolling at the same conditions but with 120 grit attached to the rotor show qualitatively the same amount of abrasive wear. These results suggest that in regime I there is negligible abrasive wear, and the kinematics of the fiber roll are, to a first approximation, given by Eq. (3), which is the requirement for normal rolling.

i

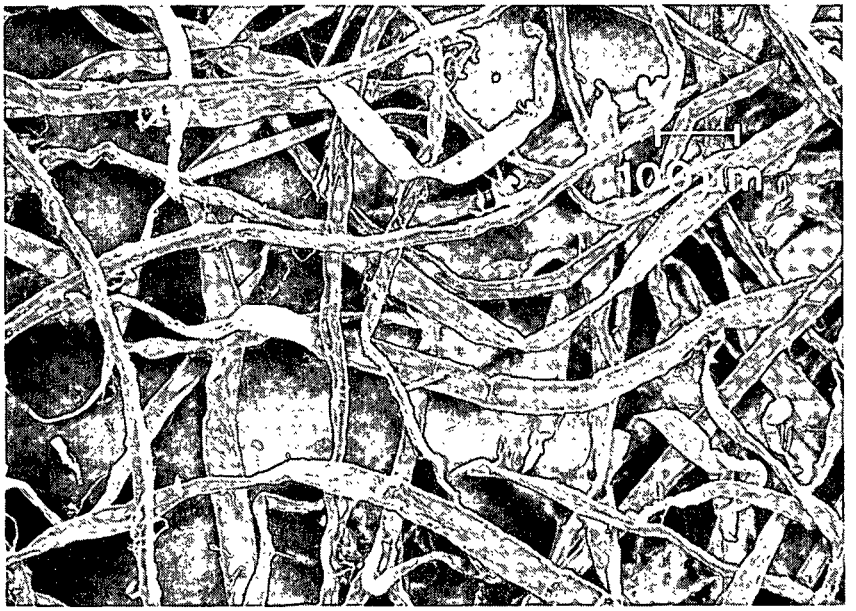

ii

Figure 7. (i) SEM photomicrograph of fibers taken from an equilibrium roll after 7 minutes of rolling; rotor speed = 70 rpm; consistency = 0.05%; plate clearance = 6.35 mm. (ii) SEM photomicrograph of pulp specimen before rolling.

ABRASIVE WEAR IN REGIME III

When regime III is realized, the suspension flow is unsteady and more than likely turbulent. Its irregular motion causes fibers or flocs of fibers to contact intermittently the rotor and stator surfaces where abrasive wear takes place. It is also possible for flocs to exhibit slip-stick behavior in regime III, i.e., for short intervals of time flocs are immobilized on the rotor and stator surfaces. Slip-stick behavior, a consequence of a variable friction force, may also result in abrasive wear. It should be noted, however, that no matter how the fibers are brought in contact with the abrading surface, the contact is always impeded by the lubricating effect of the water.

The outcome of abrasive wear is a change in fiber morphology. The type of change is dictated primarily by local flow conditions and the microstructure and physical properties of the abrading surface. Asperities of the hard surface may plow fragments from the fiber wall to form debris. The plowing action, if not too severe, may also result in external fibrillation of the fiber, i.e., the partial peeling and disruption of outer layers of the fiber. At the other extreme the plowing action may be so severe that fiber fracture or cutting occurs.

In the study of abrasive wear in regime III we have focussed principally on the plowing action of the abrasive grit that results in fiber fracture and cutting. In particular we have examined how the fiber length distribution is influenced by grit size, consistency, plate clearance, rotor speed, and shearing time. These results are presented below.

EFFECT OF ABRASIVE GRIT SIZE

Sulfite pulp was sheared for 10 minutes at 1000 rpm. The consistency and plate clearance were set at 4.4% and 2 mm, respectively. The optical photomicrographs displayed in Fig. 8 show qualitatively the effect of grit size on the abrasive wear rate. The upper left picture (A) shows untreated fibers and, at the upper right (B), fibers sheared between macroscopically smooth surfaces (no grit). The lower right (C) and the lower left (D) show results using 60 grit and 400 grit, respectively. The abrasive wear is evident as external fibrillation which increases with roughness, as the lower right photo for coarse grit clearly shows.

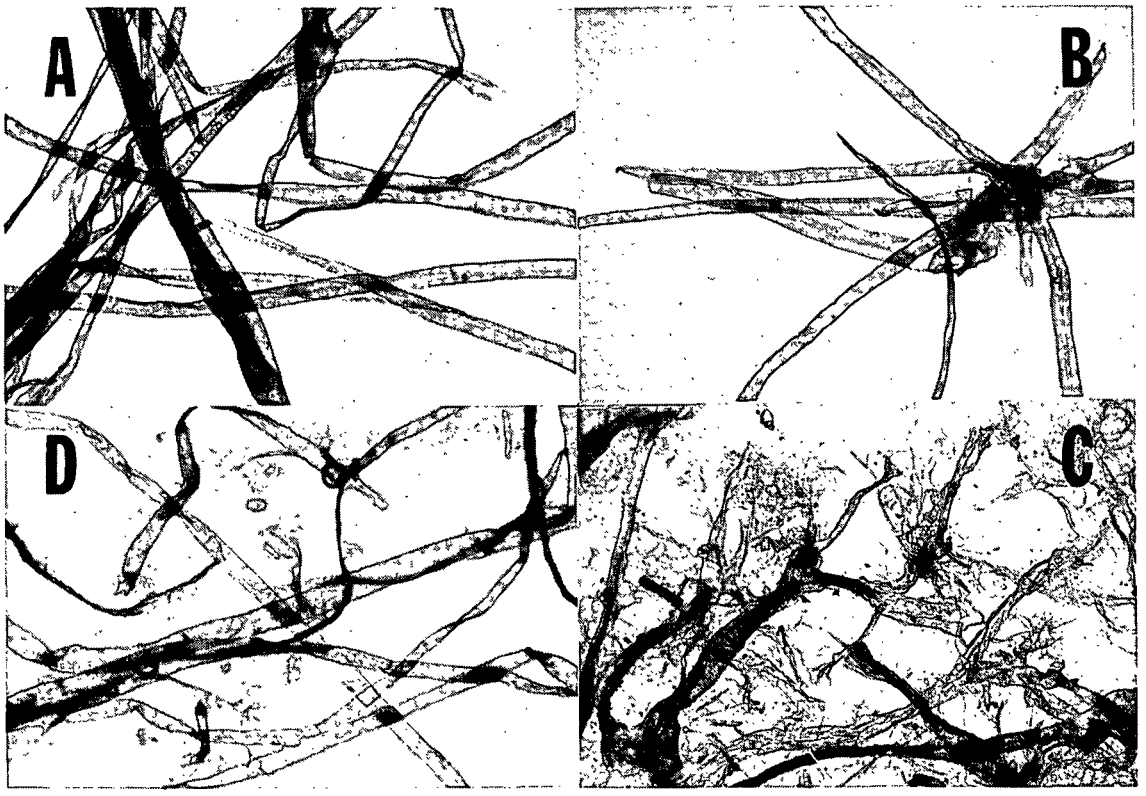

Figure 8. Photomicrographs of fibers for no shearing (A), no grit (B), 60 grit (C), and 400 grit (D) conditions.

The effect of abrasive wear on the fiber length distribution for each of the runs corresponding to the optical micrographs is shown in Fig. 9. The overall feature to note is that the distributions are shifted to shorter fibers with increasing grit size. For example, with coarse grit abrasive wear shifts the fiber length distribution substantially to fibers shorter than 2 mm and leaves no fibers longer than 3.5 mm present.

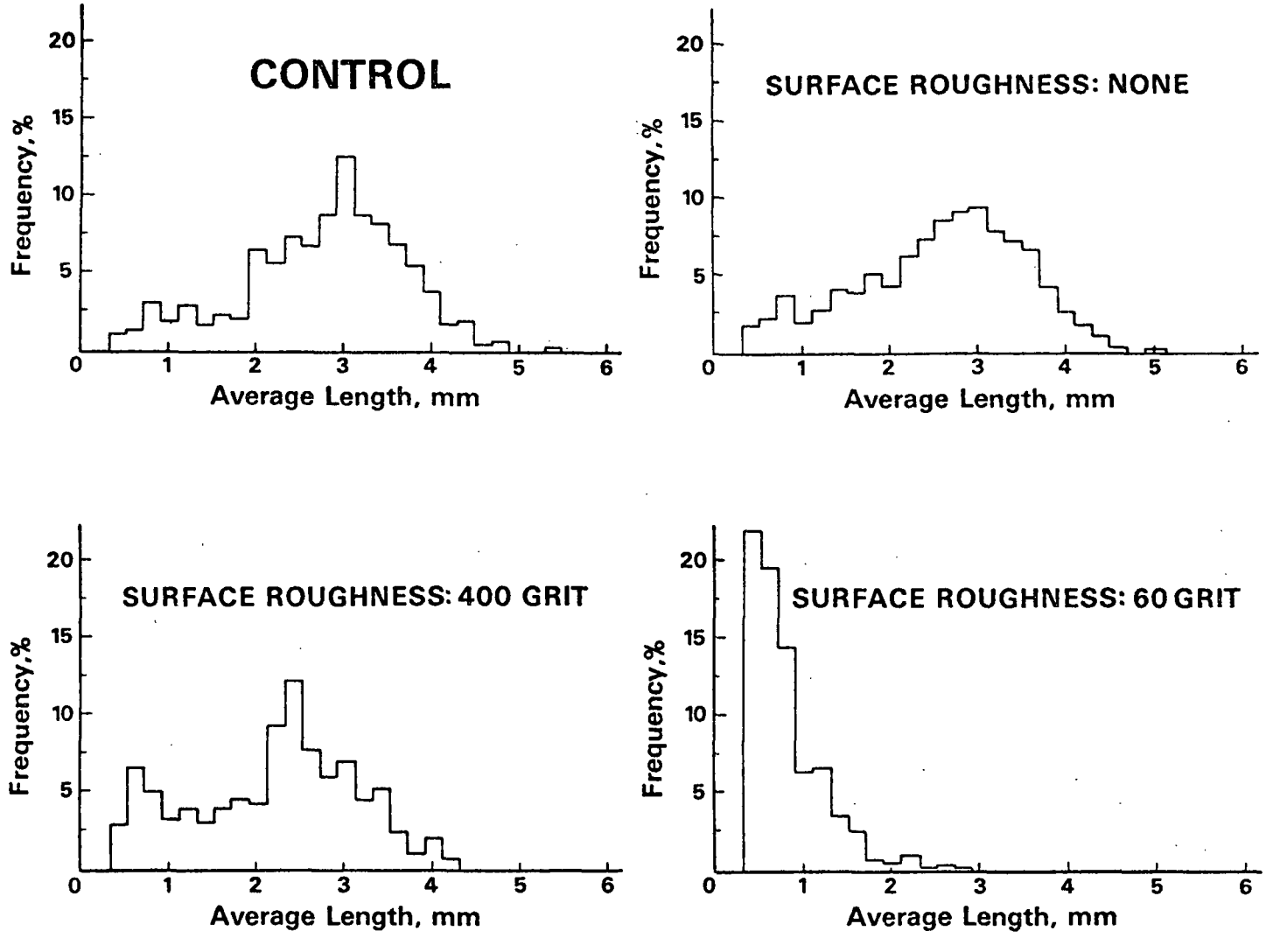

Figure 9. Fiber length distributions for fibers shown in Fig. 8.

As discussed earlier, an alternative way of representing the fiber length distribution is by its moments. When the distribution is shifted to shorter fibers, the moments are decreased. Table I lists the number-average fiber length, $\overline{L}_n$, the weight-average fiber length, $\overline{L}_w$, and the z-average fiber length, $\overline{L}_z$, for each of the distributions shown in Fig. 9. Apparently, at fixed rotor speed and consistency, grit size has little effect on the polydispersity of the distribution, as determined by the ratio $\overline{L}_w/\overline{L}_n$; this ratio remains approximately constant for each of the runs. It is evident from Fig. 8B and Table I that small changes in fiber morphology result even when the pulp is sheared in the absence of grit. Presumably the changes result from adhesive wear due to fiber-fiber and fiber-wall interactions and deformation of the fiber network effect which must always be present when pulp is subjected to shear forces.

TABLE I

FIBER LENGTH AVERAGES FOR THE DISTRIBUTIONS SHOWN IN FIGURE 9

	$\overline{L}_n$	$\overline{L}_w$	$\overline{L}_z$	$\overline{L}_w/\overline{L}_n$
Control	2.7	3.1	3.3	1.15
No grit	2.6	2.9	3.1	1.12
400 grit	2.0	2.4	3.0	1.2
60 grit	0.9	1.1	1.4	1.22

EFFECT OF SHEAR RATE

Although there is no unique shear rate that captures all the kinematics of the flows considered here, there is a shear rate that we find convenient for parameterizing the effects of abrasive wear. It is the maximum average shear rate which is based on the tangential velocity of the rotor at the chamber wall and the plate

clearance. Its convenience stems from the fact that it can be varied by changing either the plate clearance or the rotor speed, or both of them.

Before examining how abrasive wear is influenced by the maximum average shear rate, it is instructive first to show separately the effects of rotor speed and plate clearance on abrasive wear. The effects of rotor speed were examined at a consistency of 3.2%, a plate clearance of 1.9 mm, and a shearing time of 5 minutes. A 400 grit was attached to the rotor and stator surfaces and the rotor speed was varied between 300 and 1000 rpm.

In Fig. 10 the average fiber lengths are plotted against rotor speed. The asterisk denotes that the average fiber lengths have been normalized with their respective values for the untreated pulp. It is seen that the number-average fiber length decreases approximately linearly with rotor speed. Further, the difference between L_W^* and L_n^*, which is related to the polydispersity in fiber length, increases with rotor speed.

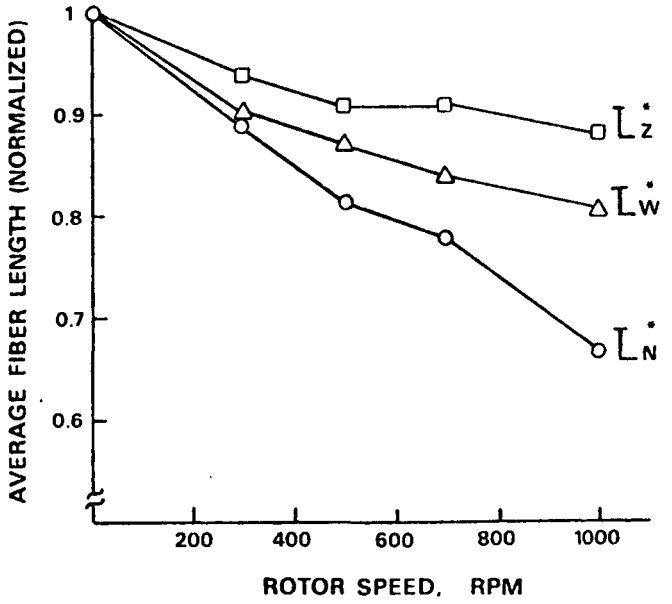

Figure 10. The effect of rotor speed on the fiber length averages; consistency = 3.2%, plate clearance = 1.9 mm, shearing time = 5 minutes, surface roughness = 400 grit.

The extent of abrasive wear is evident in the SEM photomicrographs of pulp specimens taken from pulp sheared at 500 and 1000 rpm (Fig. 11). Examples of fiber splitting, fracture, and peeling of outer layers of the fiber wall are clearly seen. Figure 12, which is a SEM photomicrograph of the 400 grit sandpaper after shearing, shows the relative dimensions of the grit and fiber.

When the effects of plate clearance were examined, the consistency, shearing time, and grit size were the same as before, but the rotor speed was 1000 rpm. The results for the number-average fiber length are shown in Fig. 13. The salient feature to note is that $\overline{L}_n$* does not vary linearly with plate clearance. However, when the data from Figs. 10 and 13 are replotted against the maximum average shear rate a linear relation is obtained over a wide range of shear rates (Fig. 14). This result is quite remarkable considering the nonuniform shear field that exists between the plates. It suggests that shear rate is a controlling parameter for abrasive wear. The weight-average fiber length and z-average fiber length were found to correlate also with the maximum average shear rate but nonlinearly.

THE EFFECT OF CONSISTENCY

When a change in consistency is accompanied by a flow regime transition, e.g., from the mobilized floc regime to the immobilized floc regime, it is not unreasonable to expect that there will be a change in the abrasive wear rate of fibers because of a change in floc mobility. However, consistency may also influence the abrasive wear rate by altering the floc size distribution in a given flow regime.

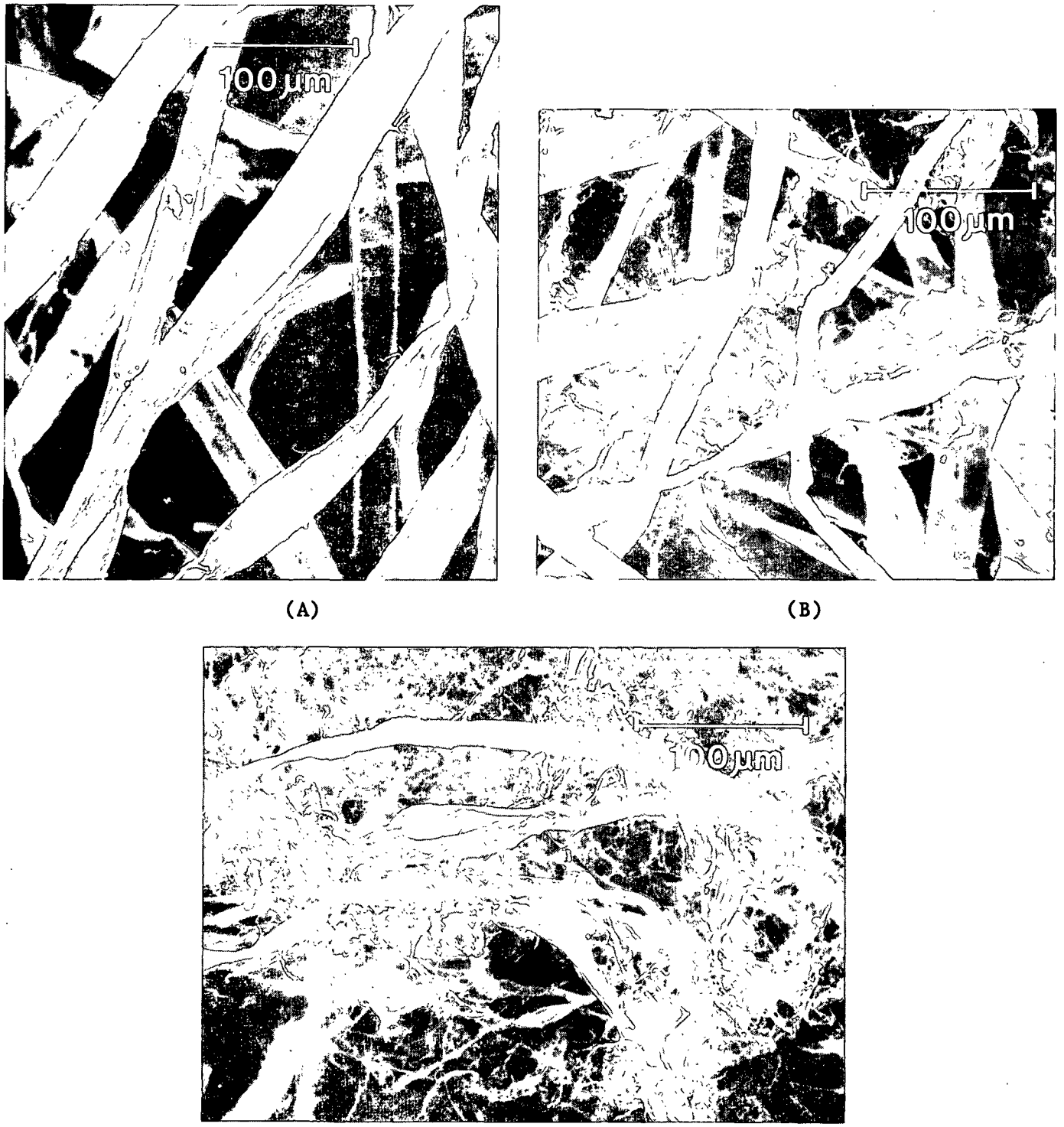

(A) (B)

(C)

Figure 11. SEM photomicrographs of unbleached sulfite softwood fibers untreated (A); sheared at 500 rpm (B); sheared at 1000 rpm (C); plate clearance = 1.9 mm, surface roughness = 400 grit, consistency = 3.2%, shearing time = 5 minutes.

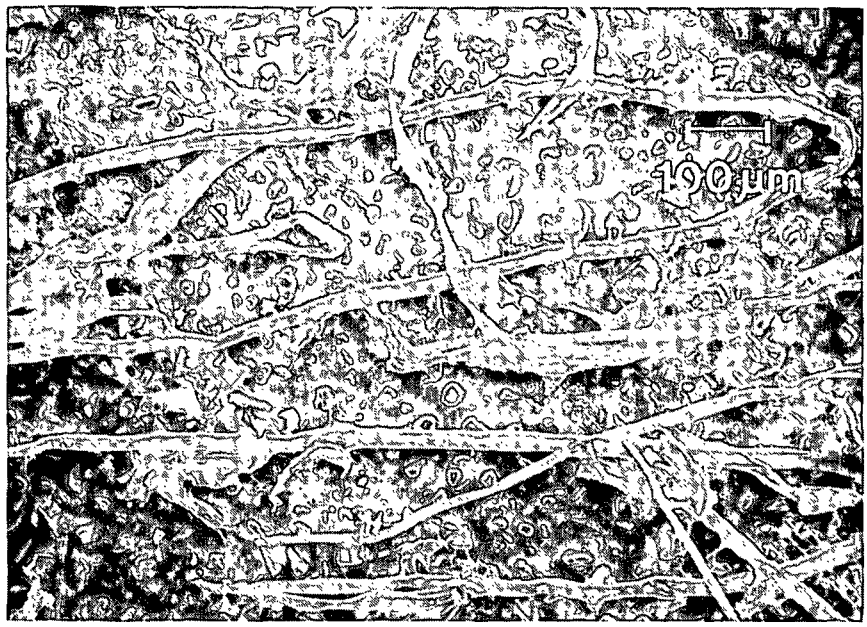

Figure 12. SEM photomicrograph of 400 grit sandpaper after shearing at 500 rpm for 5 minutes.

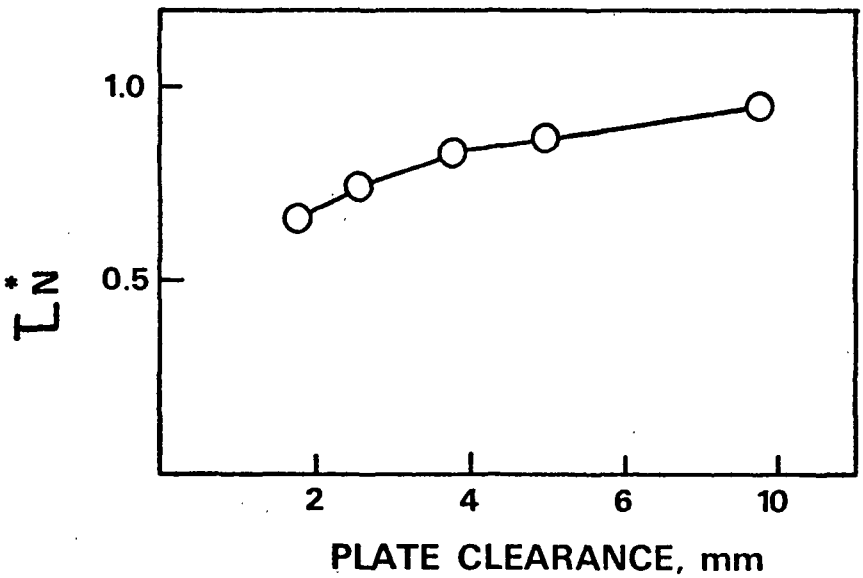

Figure 13. Variation of number-average fiber length (normalized) with plate clearance; rotor speed = 1000 rpm, consistency = 3.2%, surface roughness = 400 grit, shearing time = 5 minutes.

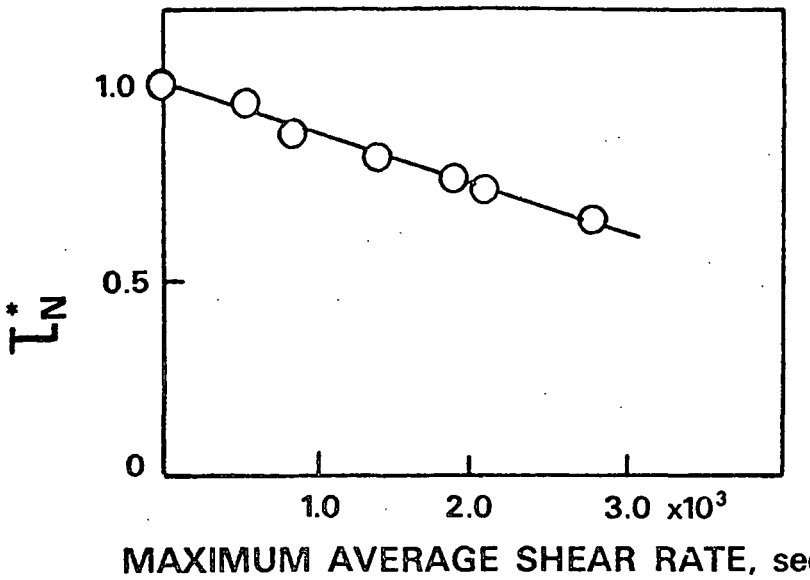

Figure 14. Variation of number-acerage fiber length (normalized) with maximum average shear rate; surface roughness = 400 grit, consistency = 3.2%, shearing time = 5 minutes.

We have investigated this effect indirectly in regime III by varying the consistency at fixed plate clearance and rotor speed. The results obtained at a plate clearance of 2.54 mm and a rotor speed of 1000 rpm are shown in Fig. 15. It is seen that for a given grit size the number-average fiber length, $\overline{L}_n$, is reduced by an increase in consistency. An almost five-fold increase in consistency results in about a 20% reduction in $\overline{L}_n$. The weight- and z-average fiber lengths, though not shown in Fig. 15, are also reduced, but the reductions are not as marked. Although $\overline{L}_n$ is reduced by increased grit size, the rate of change of $\overline{L}_n$ with consistency does not appear to be sensitive to grit size.

EFFECT OF SHEARING TIME

The results presented so far give no indication of the rate of abrasive wear or in particular how the various fiber length averages of the pulp suspension change with time. To investigate this rate process, the shearing time was varied at a given plate clearance, consistency, and rotor speed. At the commencement of each experiment new sandpaper was attached to the rotor and stator.

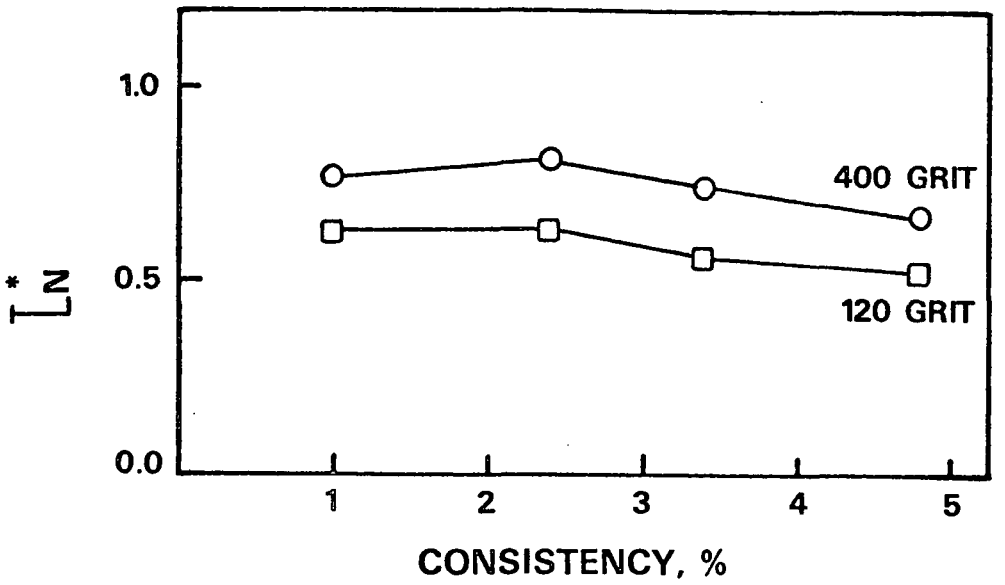

Figure 15. Variation of number-average fiber length (normalized) with consistency; plate clearance = 2.54 mm, rotor speed = 1000 rpm, shearing time = 12 minutes.

Results for two different grit sizes are shown in Fig. 16. The fiber length averages decrease rather sharply at first and then decrease more gradually. (The reason for the slight increase at 5 minutes for the 120 grit case is not known.) These results suggest that the abrasive wear rate is not constant throughout the experiment. A possible explanation for the decrease in the abrasive wear rate is the blunting of the abrasive particles with shearing time. Another possibility is that the abrasive action is impeded by debris caught between the abrasive particles, as is clearly evident in Fig. 12.

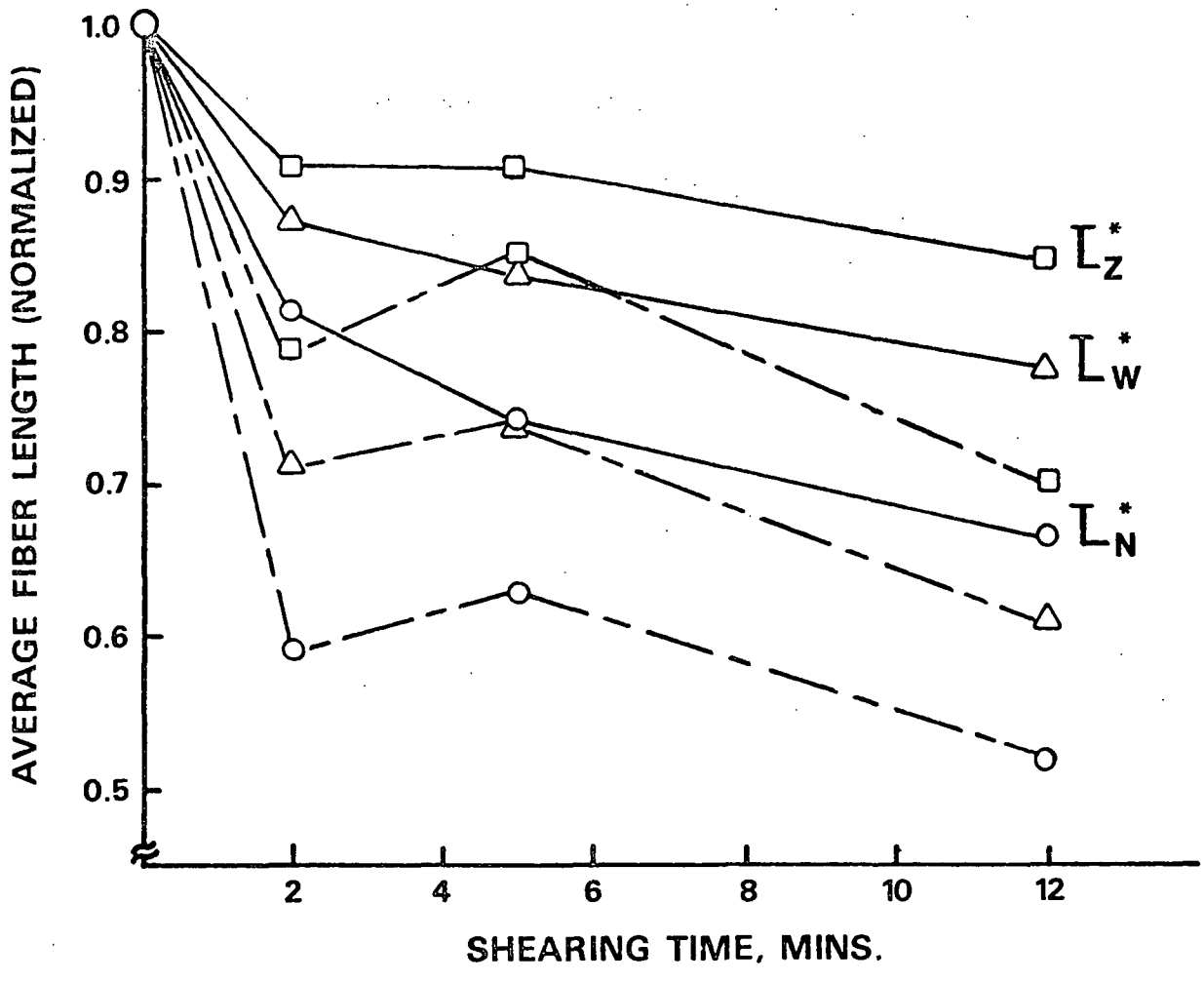

Figure 16. Variation of fiber length averages (normalized) with shearing time; plate clearance = 2.54 mm, rotor speed = 1000 rpm, consistency = 4.8%, ——— 400 grit; ----- 120 grit.

ABRASIVE WEAR AND PULP PROPERTIES

A study was undertaken to determine whether abrasive wear imparts strength properties to the pulp. In Figs. 17 and 18 strength properties of bleached softwood kraft pulp subjected to abrasive wear are plotted against sheet density. Also shown are strength properties of the same pulp refined in a 12-inch disk refiner at selected specific energies. Strength properties were determined from handsheets made according to TAPPI specifications. Details of the abrasive wear experiments are noted in Table II.

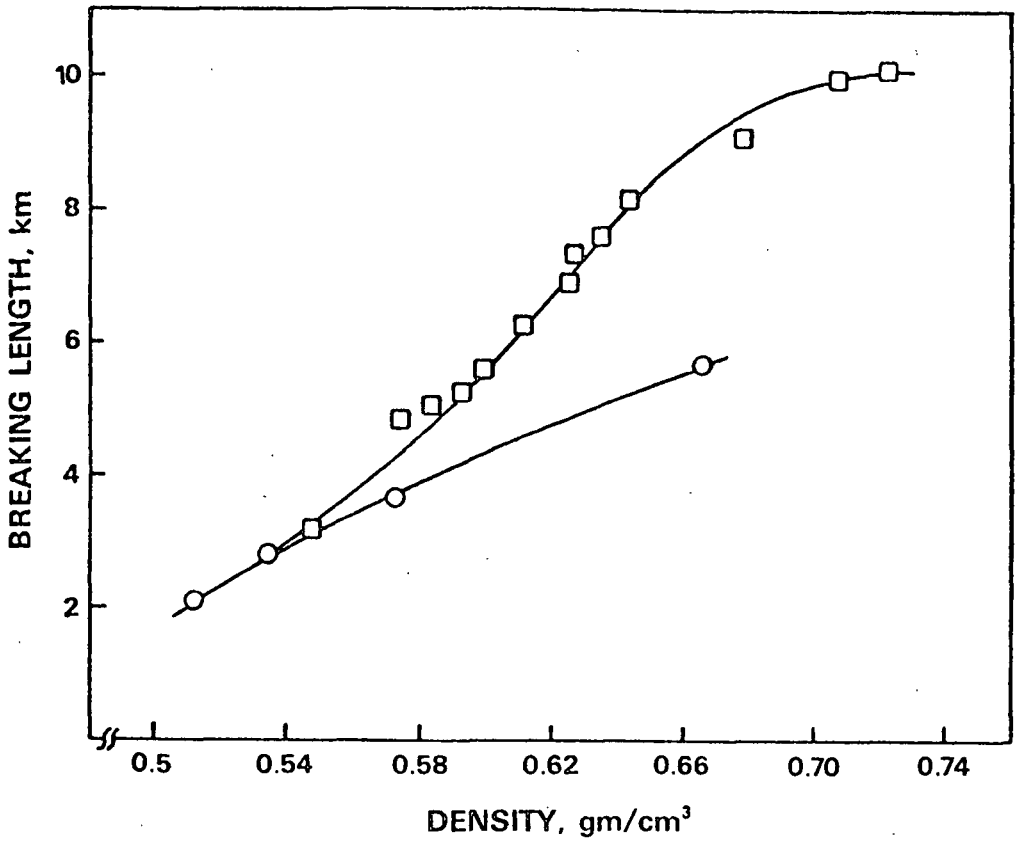

Figure 17. Breaking length development of bleached kraft softwood pulp with density; 0 abrasive wear, □ disk refining.

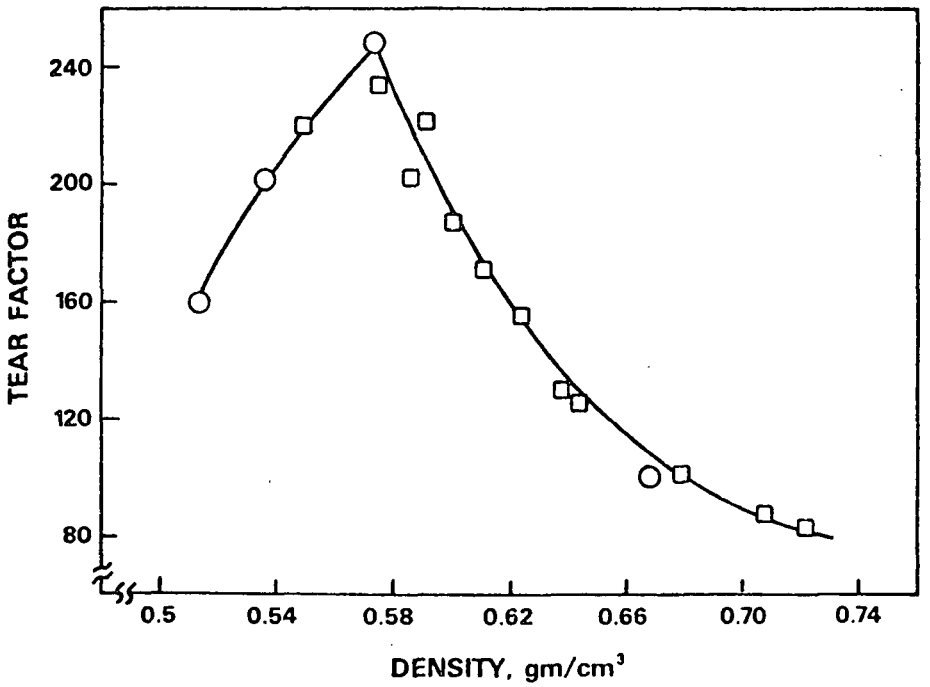

Figure 18. Tear factor development of bleached kraft softwood pulp with density; 0 abrasive wear, □ disk refining.

TABLE II

STRENGTH PROPERTIES OF PULP SUBJECTED TO ABRASIVE WEAR

Operating Conditions[a]			Handsheet Properties			
Plate Clearance (mm)	Max. Shear Rate (sec^{-1})	Consistency (%)	Density (g/cm^3)	Tear Factor	Breaking Length (km)	Light Scat. Coeff. (cm^2/g)
	C O N T R O L		0.512	160 ± 12	2.08 ± 0.08	397
5.08	1050	3.6	0.535	202 ± 6	2.82 ± 0.18	--
3.81	1410	3.1	0.573	248 ± 31	3.59 ± 0.30	377
2.54	2110	4.8	0.663	100 ± 5	5.68 ± 0.14	296

[a]Rotor speed = 1000 rpm; refining time = 5 minutes; surface roughness = 120 grit.

From Fig. 17 it is clear that abrasive wear does lead to an improvement in breaking length. But in this instance the strength potential of the pulp is not realized, since the disk refined pulp has for the most part a far superior breaking length at a given sheet density. A possible exception is at low densities (< 0.56 g/cm^3) where the pulps exhibit approximately equivalent breaking lengths. It is noteworthy that the tear-density relation is not altered by abrasive wear (Fig. 18). No attempt was made to determine the abrasive wear conditions optimal for pulp strength development.

In Fig. 19 the various fiber length averages are plotted against breaking length. Unfortunately, the fiber length distribution for the unrefined pulp was not determined. Nevertheless, it is estimated that the z-average fiber length is about 75% of the original value at the highest breaking length (or sheet density). It is unlikely that this reduction in fiber length accounts for the low breaking length of the pulp.

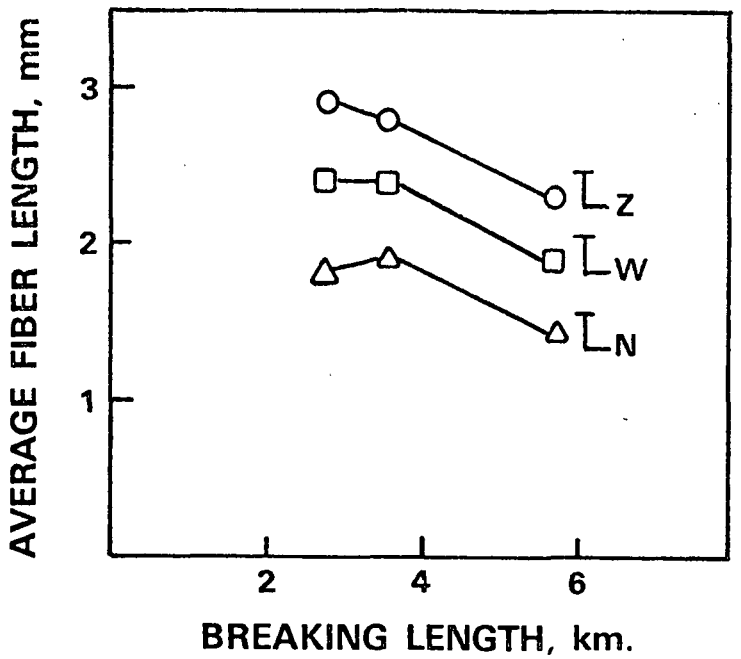

Figure 19. Fiber length averages for bleached kraft softwood pulp vs. breaking length.

LITERATURE CITED

1. J. F. Waterhouse, Tappi 53(10):1891(1970).

2. L. Westman, Svensk Papperstid. 85(4):26(1982).

3. N. K. Bridge and R. J. Hamer, Paper Tech. Ind. 18(2):37(1977).

4. F. P. Bowden, and D. Tabor, "The Friction and Lubrication of Solids, Part 11," Oxford University Press, 1964.

5. J. P. Casey, "Pulp and Paper, Vol. 11," Interscience Publishers, N.Y., 1961.

6. D. Wahren, Svensk Papperstid. 67(13):536(1964).

7. E. Rabinowicz, "Friction and Wear of Materials," John Wiley & Sons, N.Y., 1965.

8. D. Atack, "Fibre-Water Interactions in Papermaking," Transactions of the Symposium held at Oxford, September, 1977. (Edited by the Fundamental Research Committee.) Technical Division of the British Paper and Board Industry Federation, London 261, 1978.

9. B. G. Norman, K. Moller, R. Ek, and G. G. Duffy, "Fibre-Water Interactions in Papermaking," Transactions of the Symposium held at Oxford, September, 1977. (Edited by the Fundamental Research Committee) Technical Division of the British Paper and Board Industry Federation, London 195, 1978.

10. J. d'A. Clark, "Pulp Technology and Treatment for Paper," Miller Freeman Publishers, Inc., San Francisco, 1978.

11. A. A. Robertson and S. G. Mason, Tappi 40(5):326(1957).

12. K. R. Symon, "Mechanics," 3rd Edition, Addison-Wesley Publishing Co., 1971.

13. W. D. May, E. L. Morris, and D. Atack, J. Applied Physics 34:1920(1963).

THE INSTITUTE OF PAPER CHEMISTRY

*Brian G. Higgins
Research Associate
Papermaking Group
Engineering Division

Clyde H. Sprague
Director
Paper Materials & Systems Division

*Now with: Department of Chemical Engineering,
University of California at Davis.